EVS27
Barcelona, Spain, November 17-20, 2013

Analysis of Degradation Mechanism of Lithium Iron Phosphate Battery

Genki KANEKO[1], Soichiro INOUE[1], Koichiro TANIGUCHI[1], Toshio HIROTA[1],
Yushi KAMIYA[1], Yasuhiro DAISHO[1], Shoichi INAMI[2]

[1]*Waseda University, 55S-704, 3-4-1 Okubo, Shinjuku-ku, Tokyo, JAPAN, genkikaneko@suou.waseda.jp*
[2]*MITSUI ENGINEERING & SHIPBUILDING CO.LTD, 5-6-4 Tsukiji, Chuo-ku, Tokyo, JAPAN*

Abstract

The degradation mechanisms of lithium iron phosphate battery have been analyzed with 150 day calendar capacity loss tests and 3,000 cycle capacity loss tests to identify the operation method to maximize the battery life for electric vehicles. Both test results indicated that capacity loss increased under higher temperature and SOC conditions. And also, large increase of internal resistance on the high temperature and high SOC conditions was confirmed by AC impedance tests. The real cycle capacity loss characteristic was derived by subtracting the capacity decrease due to calendar capacity loss during the cycle test from the overall capacity loss characteristic obtained from the cycle test. As a result, it is found that the real capacity loss contains not only structural disorders of electrode but also degradation factors due to the chemical reactions. Characteristics of degradation were quantified with equations based on the chemical kinetics. With this degradation prediction, an operation method was proposed that is compatible with the long life of batteries and the safety driving of a vehicle. As a result, with optimizing the SOC range used in the operation as follows: 30-10% in the warm seasons, 45-25% in the cold seasons, it was found that batteries can last 4 times longer than it used with high SOC range in every season.

Keywords: lithium battery, battery calendar life, BEV (battery electric vehicle)

1 Introduction

In recent years, battery electric vehicles (BEVs) have been actively developed and introduced to the market. BEVs have superior environmental performance because emit no CO_2 and other gases while driving. However, in terms of more popularization of BEVs, weaknesses for cruising range, cost of batteries and user-friendliness of charging remain major challenges. To resolve these issues, a concept "short range driving and very frequent charging" was formulated [1]. Under this approach, the authors developed the short-range frequent-recharging electric vehicles (Figure 1) and studied methods of greatly reducing the number of large, heavy, and expensive batteries. In addition, researching about non-contact inductive power supply (IPS) system was developed as a way of improving charging convenience, and a lithium iron phosphate battery was developed suit to rapid charging [2]. Especially about batteries, a lot of efforts have been put into analyzing its degradation mechanisms. Up to now, our research group has been made various studies about batteries for BEVs [3]. By analyzing the degradation mechanism of batteries, it could be possible to

obtain guiding principles for next generation batteries and indicate how to last the life of batteries. Also, battery degradation causes problems such as decline of cruising range and decrease of power. In the scope of safety operation, it is significant that controlling the progressing of battery degradation. The aim of this paper is to contribute the longevity of BEVs with addressing the operation method to realize the coexistence vehicle's safety operation and battery's long life.

(a) WEV-0 adv.

(b) WEV-1

(c) WEB-3

Figure1: Short-range Frequent-recharging Electric Vehicles

2   Evaluation Tests

2.1   Degradation Factors

Degradation factors of lithium-ion batteries have been reported by previous researches [4] [5]. Figure 2 shows the waste of lithium-ion comes from formation of solid electrolyte interface (SEI). Formation of SEI is the dominant degradation factor in the calendar capacity loss. Figure 3 shows the structural disorder of the

electrode as lithium-ion goes in and out of the electrode. Structural disorder is progressing with the discharge and charge processes. Furthermore, acceleration of wasting lithium-ion with the discharge and charge processes could be the factor of degradation in the cycle processes. Temperatures, state of charge (SOC) and SOC range in the tests were extracted as external factors that have impacts on degradation.
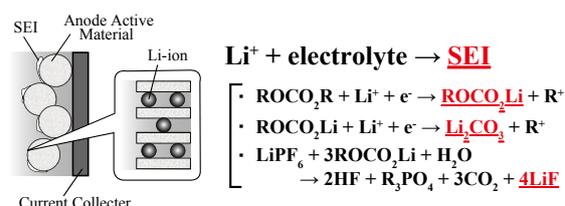

$$Li^+ + electrolyte \rightarrow SEI$$

- $ROCO_2R + Li^+ + e^- \rightarrow ROCO_2Li + R^+$
- $ROCO_2Li + Li^+ + e^- \rightarrow Li_2CO_3 + R^+$
- $LiPF_6 + 3ROCO_2Li + H_2O$
  $\rightarrow 2HF + R_3PO_4 + 3CO_2 + 4LiF$

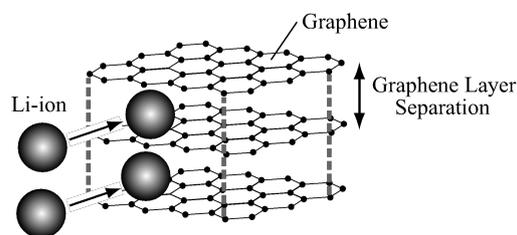Figure2: SEI Reaction Model

Figure3: Structural Disorder Model

2.2   Calendar Capacity Loss Tests

Figure4: Test Battery Cell

Table1: Test Battery Specification

Cathode Material	$LiFePO_4$
Anode Material	C_6 (Graphite)
Rated Voltage	3.25 V
Rated Capacity	6.2 Ah
Dimensions (mm)	L120×W3×H140

Figure 4 and Table 1 show the specification of the test battery cell. Lithium iron phosphate battery is known for its superiority of safety and manufacturing cost. Test battery cell is laminate

type cell, has superior rapid charging performance and is suitable for electric vehicles designed to be charged frequently and driven short distances between charges. Parameters for the calendar capacity loss tests are temperature(5℃，25℃，45℃) and SOC(90%, 50%, 10%). Figure 5 shows the results of the calendar capacity loss tests. These results indicated that the capacity loss increased under the higher temperature and SOC conditions. It is thought that the main cause of this large capacity loss is that the reactions between the lithium ion and the electrolyte are accelerated under high temperature and SOC conditions. As a result, the absolute amount of lithium ions decreases due to the growth of SEI films.
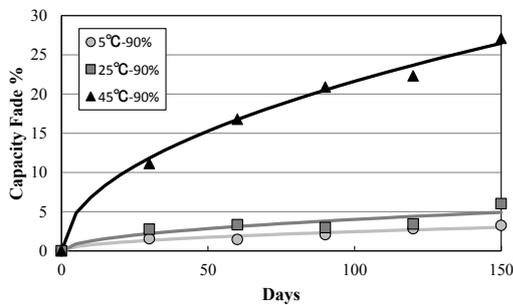
(a) Temperature Dependency
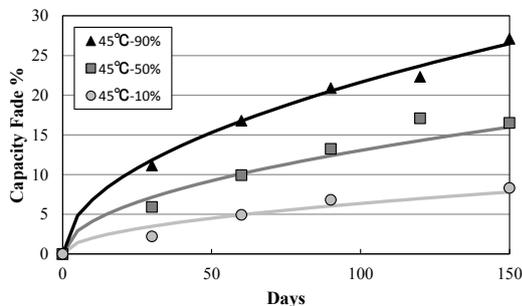
(b) SOC Dependency

Figure5: Calendar Capacity Loss Test Results
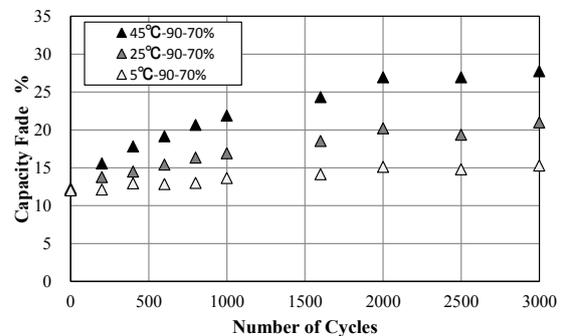
2.3   Cycle Capacity Loss Tests

Table 2 shows the condition of cycle capacity loss tests. For the cycle tests, the cell was discharged from each start SOC and charged to the start SOC. The charge rate is 2.4C (14.88A) and the discharge rate is 1.2C (7.44A). Also after charging, 5 minutes rest has set to avoid sudden temperature rise. Charge/discharge amount is 1.24Ah that equivalent to 20% SOC of test cell. Charge/Discharge rate and Amount Ah of a cycle are determined by assuming the operation way of

WEV-1. The cut-off voltage for the cycle tests and capacity measurement tests were at 4.0V and 2.0V. Capacity measurement test was carried out on the condition of 25℃. Parameters for the cycle tests are temperature (5℃, 25℃, 45℃) and SOC range (90-70%, 70-50%, 40-20%). Test battery cell is same type one used in the calendar capacity loss tests, expect has about 12% of initial capacity loss in the cause of 900 day, 100 cycle running tests.

Table2: Cycle Test Condition

Temperature	5℃, 25℃, 45℃
SOC range	90-70% 70-50% 40-20%
Charge/Discharge Rate	14.88A/7.44A
Charge/Discharge Amount	1.24Ah/1.24Ah

Figure 6 shows the results of the cycle capacity loss tests. These results confirmed that capacity loss increased under the higher temperature and SOC conditions. On the other hand, in the 40-20% SOC range test, we found that capacity loss in 5℃ was larger than 25℃. These results indicated that cycle capacity loss includes both degradation due to the chemical reaction and structural disorder.

(a) Temperature Dependency
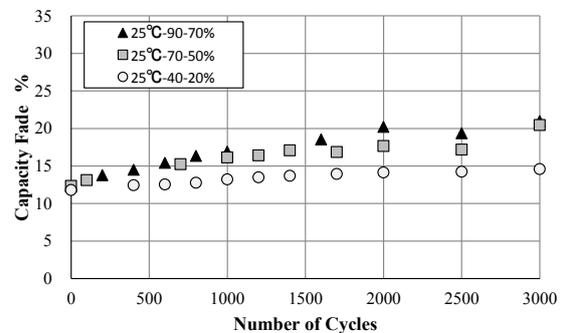
(b) SOC Dependency

Figure6: Cycle Capacity Loss Test Results

2.4   AC Impedance Tests

AC impedance tests were carried out to analyze the degradation of test battery cell. AC impedance test is one of the transient measurement methods that impedance and admittance could be calculated by measuring the response to the micro AC signal applied to the battery. An equivalent circuit shown in Figure 7 was used for analyzing the impedance spectrums. L is inductor factor of measurement systems, R_{sol} is resistance of electrolyte, R_{ct} is resistance of moving electric charge, Z_w is Warburg impedance of diffusion, CPE is kind of an electric double-layer capacity that expresses elliptic distortion of plots [6]. This circuit was selected to fit the measured impedance spectrum.
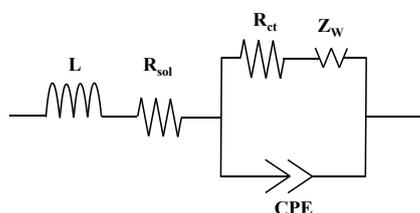

Figure7: Equivalent Circuit of Test Battery Cell

All tests were carried out on the condition of discharge at 50% SOC, frequency range between 0.1 and 10k Hz. Figure 8 shows the cole-cole plots of test batteries. These plots contain both cathode and anode reactions. Shifting of the cole-cole plots along the axis Z' indicates increase of the R_{sol}, and also expand of radius of the semicircle indicates increase of the R_{ct}. Increase of the R_{sol} has shown significantly under high temperature and SOC conditions. This is speculated to cause of grown SEI films and could be the main factor of degradation. And also a little increase of the R_{ct} has shown under high temperature and SOC conditions. This is speculated to cause of structural disorder of electrode. Increase of internal resistance attend to capacity fade has confirmed by evaluating absolute amount of R_{sol} and R_{ct}.
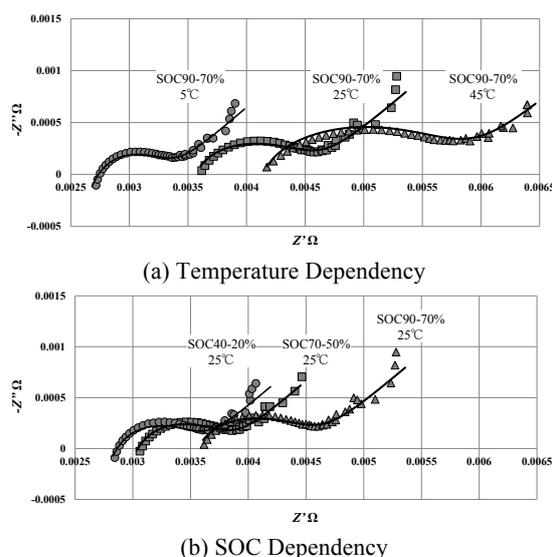

(a) Temperature Dependency

(b) SOC Dependency

Figure8: Cole-Cole Plots of Test Battery Cells

3   Discussion

3.1   Calendar Capacity Loss

Figure5 suggests that chemical reactions are the main cause of calendar capacity loss. Therefore, characteristics of calendar capacity loss were quantified with the equation based on the chemical kinetics. Previous research has suggested that capacity loss is relevant to the amount of grown SEI films. A simple model for generation of SEI films is represented by the equation (1). The reaction rate of equation (1) moves from equilibrium state is quantified with the equation (2).

$$\text{Li} + \text{electrolyte} + e^- \rightarrow SEI \qquad (1)$$
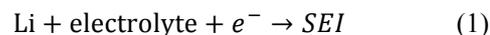
$$v_0 = A'[Li^+]e^{-\frac{E_a}{RT}} \qquad (2)$$

Where A' is frequency factor, E_a is activation energy, R is gas constant, and T is ambient temperature.

While terminal voltage rises by ΔV from equilibrium state, the electric potential of anode drops by ΔE and potential energy of electron on the surface of anode drops by $F\Delta E$. This variation of potential energy becomes the motive force of reduction reaction which generates SEI films. Activation energy drops by $(1-\beta)F\Delta E$. Reaction rate equation while the terminal voltage rises by ΔV is quantified with the equation (3).

$$v = A'[Li^+]e^{-\frac{E_a-(1-\beta)F\Delta E}{RT}} \qquad (3)$$

$\Delta V = V$ could be completed where reference voltage V_0 is defined as 0V. To simplify the equation, here suppose that $\Delta E \propto \Delta V = V$. Equation (3) could be expressed as equation (4) if the consistency of li-ion is proportional to the SOC.

$$v = A(SOC)e^{-\frac{E_a-\alpha V}{RT}} \qquad (4)$$

Each coefficients A, E_a, α are determined with curve fitting techniques. Characteristics of calendar capacity loss were quantified with equation (5).

$$\left\{ \begin{array}{l} \text{Deduction coefficient of capacity} \\ \text{due to the calendarcapacity loss} \\ \qquad (\%) = k_s * t^{0.5} \\ \\ k_s = 4475 * (SOC) \\ \qquad * exp\left(-\frac{49767-811V}{RT}\right) \end{array} \right. \qquad (5)$$

The variable k_s in the equation is defined as the calendar capacity loss coefficient.
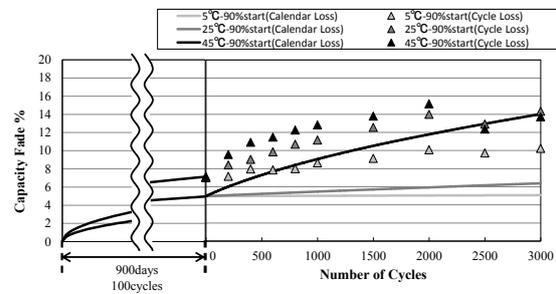
3.2   Cycle Capacity Loss

The calendar capacity loss progresses even at the cycle capacity loss tests. The real cycle capacity loss characteristic was derived by subtracting the capacity decrease due to calendar capacity loss during the cycle test from the overall capacity loss characteristic obtained from the cycle test. Figure 7 shows that the real capacity loss progresses linearly with the square loot of the number of days of cycles. From the temperature and SOC dependency showed in Figure 7, it is suggested that the real capacity loss contains not only structural disorder but also a factor due to the chemical reactions. Separation and regeneration of SEI films progressing with the charge and discharge processes are speculated to be the cause of this chemical reaction. Characteristics of cycle capacity loss were also quantified with the equation (6) based on the mechanical disorder and chemical kinetics.
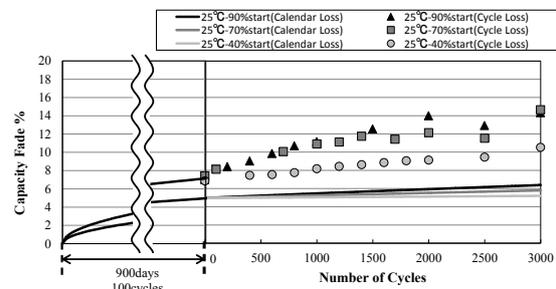
$$\left\{ \begin{array}{l} \text{Deduction coefficient of capacity} \\ \text{due to the cycle capacity loss} \\ \qquad (\%) = k_c * N^{0.5} \\ \\ k_c = 394.1 * (SOC) \\ \qquad * exp\left(-\frac{31013-0.01734V}{RT}\right) \\ \qquad + k_{c\,mechanical} \end{array} \right. \qquad (6)$$

Where N is cycle number, k_c is defined as the cycle capacity loss coefficient. $K_{c\,mechanical}$ is fixed number shown in equation (7).

$$K_{c\,mechanical} = 0.154 \, (5\,℃), 0.0855 \, (25\,℃, \ 45\,℃) \qquad (7)$$

(a)Temperature Dependency

(b)SOC Dependency

Figure7: Real Capacity Loss in Cycle Tests

3.3   Optimization of the BEV's Operation Method

The results of calendar tests and cycle tests showed that it is desirable using in low SOC range to reduce the capacity decrease under every temperature conditions. On the other hand, an operation with low SOC range has a risk of reaching the lower limit of supply voltage especially at low temperatures because of increasing of the internal resistance. The operation of the WEV-1 was optimized with degradation

predictions. WEV-1 was developed as a transfer tool in a vast tract of site such as premises of university or factory. Its assumed operation way is 5 round trips a day with a route consuming electric power equivalent to 20% of SOC. In this operation way, the SOC range used in the operation was optimized by seasons as follows: 30-10% in the warm seasons, 45-25% in the cold seasons. Considering the increasing of internal resistance of batteries, used SOC range in the cold seasons was set to be higher than it in the warm seasons. The life of battery was set to 70% capacity retention of fresh battery. As a result, it was found that batteries can last 4 times longer than it used with high SOC range in every season (Figure 8).
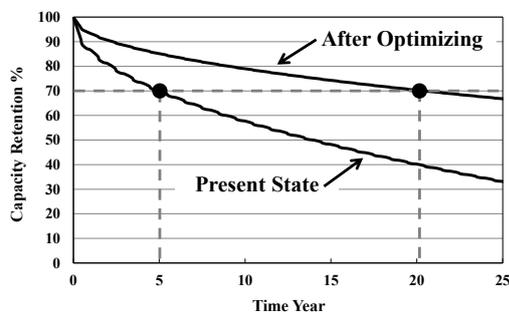

Figure8: Life Time Prediction of Present State and After Optimizing State

4   Conclusion

Degradation mechanisms of lithium iron phosphate battery were analyzed and an operation method of BEV was optimized with the degradation prediction. The obtained results are as follows:

(a) 150 day calendar capacity loss tests have been carried out. Experimental results showed that calendar capacity loss increased under the higher temperature and SOC conditions, and progresses linearly with the square root of time. From the results, it could be said that calendar capacity loss is caused by chemical reactions. Formation of SEI films is thought to be the dominant factor. Calendar capacity loss characteristics were quantified with an equation based on the chemical kinetics.

(b) 3,000 cycle capacity loss tests have been carried out. Experimental results showed that calendar capacity loss progresses linearly with the square root of cycle numbers. From the

results, it could be said that cycle capacity loss includes both degradation due to the chemical reaction and structural disorder.

(c) The real cycle capacity loss characteristic was derived by subtracting the capacity decrease due to calendar capacity loss during the cycle test from the overall capacity loss characteristic obtained from the cycle test. As a result, the real capacity loss also progressed linearly with the square root of cycles. From the results, some chemical reactions were thought to be included in the real cycle capacity loss. Separation and regeneration of SEI films progressing with the charge and discharge processes are speculated to be the cause of this chemical reaction. The real cycle capacity loss characteristics were quantified with an equation with the mechanical disorder and chemical kinetics.

(d) With degradation predictions, an operation method was proposed that is compatible with the long life of batteries and the safety driving of a vehicle. As a result, with optimizing the SOC range used in the operation as follows: 30-10% in the warm seasons, 45-25% in the cold seasons, it was found that batteries can last 4 times longer than it used with high SOC range in every season.

In addition, large capacity loss was seen in the cycle capacity loss tests on the condition of low temperature and low SOC range. A detailed analysis on structural disorder characteristic under low temperature condition will be presented in a future paper.

Acknowledgements

References

[1]   Y. Kamiya, Y. Daisho, et al: "Development and performance evaluation of an advanced electric micro bus transportation system - Development and performance evaluation of Waseda advanced Electric micro Bus (WEB)", -Review of Automotive Engineering (JSAE) , Vol. 28, No. 2, pp. 259- 266. (2007)

[2]   F. Yoshida, et al.: "Development of short-range frequent-recharging small electric

vehicle equipped with non-contact inductive power supply system and LiFePO4 lithium-ion battery", Proceedings of the IEEE VPPC 2010, conference DI-1-6, pp. 1-3(CD-ROM) (2010)

[3] K. Nunotani, et al.: "Development and performance evaluation of lithium ion phosphate battery with superior rapid charging performance - Second report: Evaluation of battery capacity loss characteristics", -Proceedings of the IEEE VPPC 2011 conference, ISBN978-1-61284-246-9, CFP11VPP-USB, PS-52, pp. 1-4. 2011. 9

[4] Hiroaki Yoshida, et al.: "Capacity Loss Mechanism of Space Lithium-Ion Cells and Its Life Estimation Method", Electrochemistry, vol.71, No.12, pp.1018-1024 (2003)

[5] Zempachi Ogumi: "Surface Film Formation on Graphite Negative Electrode for Lithium Ion Batteries - Analysis by SPM", GS Technical Report, vol.62, (2003)

[6] Andreas Jossen: "Fundamentals of battery dynamics", Journal of Power Sources, 154, 530-538 (2006)

Authors

Genki Kaneko
Waseda University, 55S-704, 3-4-1 Ohkubo, Shinjuku-ku, Tokyo, JAPAN
Tel:+81-3-5286-3123
Email : genkikaneko@suou.waseda.jp
G. Kaneko received a B.Eng. degree from Tokyo Metropolitan University, and is currently studying for a M.Eng. degree at Waseda University.

Soichiro INOUE
Waseda University, 55S-704, 3-4-1 Ohkubo, Shinjuku-ku, Tokyo, JAPAN
Tel:+81-3-5286-3123
S. Inoue received B.Eng. and M.Eng. degrees from Waseda University, and is currently an engineer of electronics.

Koichiro TANIGUCHI
Waseda University, 55S-704, 3-4-1 Ohkubo, Shinjuku-ku, Tokyo, JAPAN
Tel:+81-3-5286-3123
Email:koh-taniguchi@fuji.waseda.jp
K. Taniguchi received a B.Eng. degree from Waseda University, and is currently studying for a M.Eng. degree at Waseda University.

Toshio HIROTA
Waseda University, 55S-704, 3-4-1 Ohkubo, Shinjuku-ku, Tokyo, JAPAN
Tel:+81-3-5286-3123
T. Hirota received a doctorate of Engineering from Hokkaido University, and is currently a visiting professor at Waseda University.

Yushi KAMIYA
Waseda University, 55S-704, 3-4-1 Ohkubo, Shinjuku-ku, Tokyo, JAPAN
Tel:+81-3-5286-3123
Email:kamiya@waseda.jp
Y. Kamiya obtained B.Eng. and M.Eng. degrees and received a doctorate of Engineering from Waseda University, and is currently a professor at Waseda University.

Yasuhiro DAISHO
Waseda University, 58-226, 3-4-1 Ohkubo, Shinjuku-ku, Tokyo, JAPAN
Tel:+81-3-5286-3253
Email:daisho@waseda.jp
Y. Daisho graduated the doctor's course of Waseda University. He is currently a professor at Waseda University.

Shoichi INAMI
MITSUI ENGINEERING & SHIPBUILDING CO.LTD, 5-6-4 Tsukiji, Chuo-ku, Tokyo, JAPAN
S. Inami received the B.Eng. degree from Kobe University, and is currently an engineer of mechanics at MITSUI ENGINEERING & SHIPBUILDING CO.LTD